Workshop on Fission Dynamics

Chongqing, China, 11-15 May 2026

From Fusion and Quasifission to Fission within TDDFT

Lu Guo

University of Chinese Academy of Sciences, Beijing, China

Outline

- Introduction
- Time-dependent Hartree-Fock
- Microscopic Dynamics
  - Fusion
  - Quasifission
  - induced Fission
- Summary and Perspectives

Topical Review:

C. Simenel, Lu Guo and K. Sekizawa, Annu. Rev. Nucl. Part. Sci. 76, *** (2026)

Liang Li and Lu Guo, J. Phys. G (in preparation)

Xiang-Xiang Sun and Lu Guo, Comm. Theor. Phys. 74, 097302 (2022)

Background

- Heavy-ion collisions：three steps of SHE and competing reaction mechanisms
  - cold fusion: using ^{208}Pb (^{209}Bi) as target, the heaviest SHE is up to Z=113 so far
  - hot fusion: using ^{48}Ca as projectile, the heaviest is up to Z=118 so far
- Quasifission and fusion-fission are the primary mechanism in preventing SHE formation
- Fusion probability is several orders of magnitude difference among the different phenomenological models

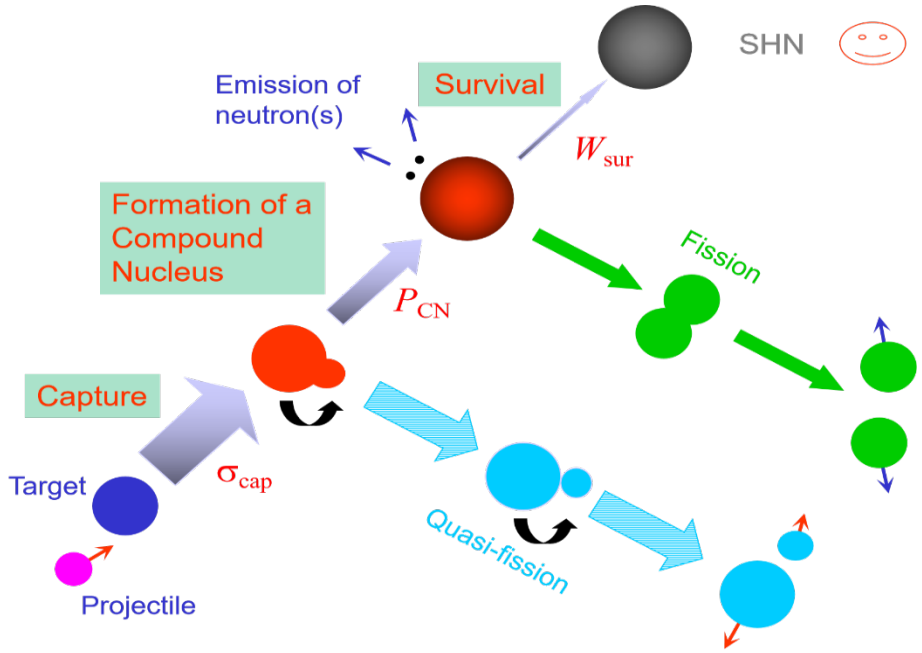

Shan-Gui Zhou, Nucl. Phys. Rev 34, 318 (2017)

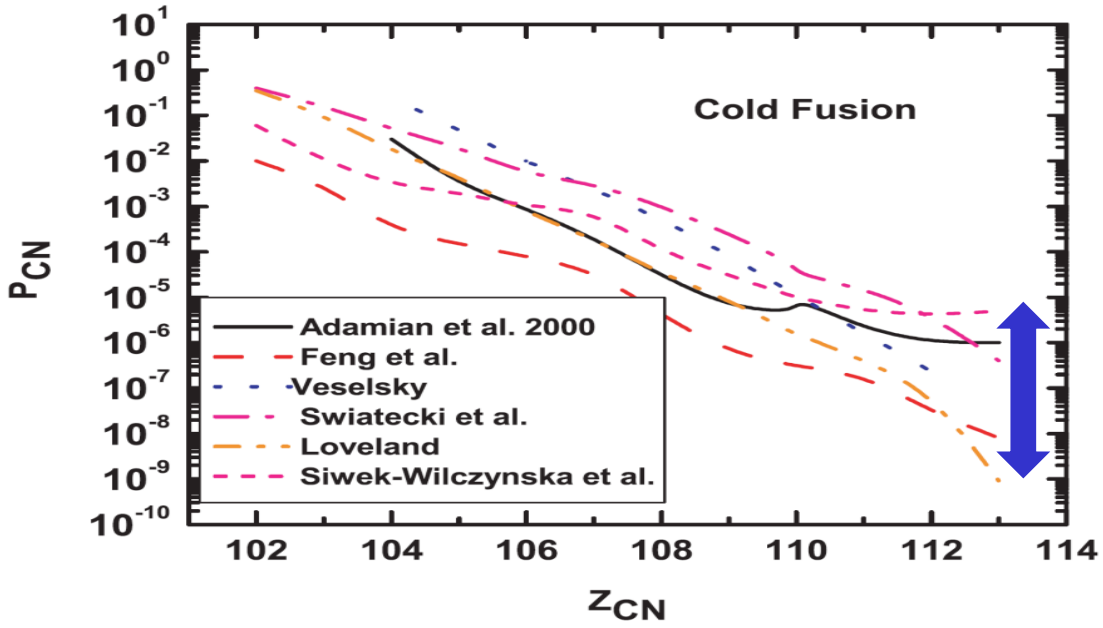

R. S. Naik et al, Phys. Rev. C76, 054604 (2007)

time-dependent Hartree-Fock

$$S = \int_{t_1}^{t_2} \left\langle \Psi(t) \mid H - i\hbar\partial_t \mid \Psi(t) \right\rangle dt, \qquad H = \sum_{i=1}^{A} t_i + \sum_{i<j}^{A} v_{ij}$$

$$\Psi(\mathrm{r}_1, r_2, \cdots, r_A, t) = \frac{1}{\sqrt{A!}} \det\left|\varphi_\lambda(r_i, \mathrm{t})\right|, \qquad i\hbar\frac{\partial\varphi_\lambda}{\partial t} = h\varphi_\lambda$$

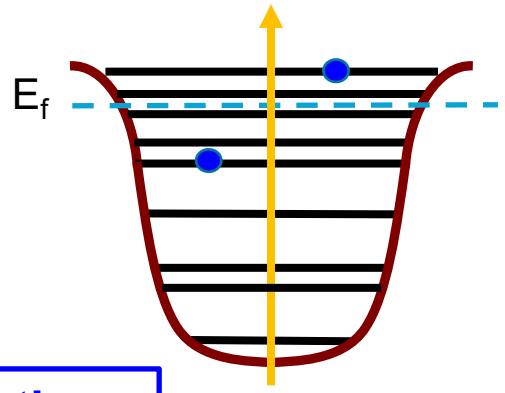

3D Lattice: no spatial symmetry restrictions

Advantages:

- **Nuclear structure and reactions in a unified framework (same EDF);**
- **Dynamical and quantum effects are automatically incorporated;**
- **No adjustable parameters for the dynamics**

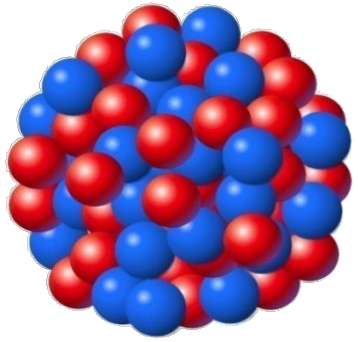

Limitations:

- **Quantum tunneling is missing;**

Lu Guo, J. A. Maruhn, and P. G. Reinhard, Phys. Rev. C 76, 014601 (2007)
Lu Guo, J. A. Maruhn, and P. G. Reinhard, Phys. Rev. C 77, 041301(R) (2008)
P. G. Reinhard, Lu Guo, and J. A. Maruhn, Eur. Phys. J. A 32, 19 (2007)

time-dependent Hartree-Fock

$$S = \int_{t_1}^{t_2} \left\langle \Psi(t) \left| H - i\hbar\partial_t \right| \Psi(t) \right\rangle dt, \qquad H = \sum_{i=1}^{A} t_i + \sum_{i<j}^{A} v_{ij}$$

$$\Psi(\mathrm{r}_1, r_2, \cdots, r_A, t) = \frac{1}{\sqrt{A!}} \det\left|\varphi_\lambda(r_i, \mathrm{t})\right|, \qquad i\hbar\frac{\partial\varphi_\lambda}{\partial t} = h\varphi_\lambda$$

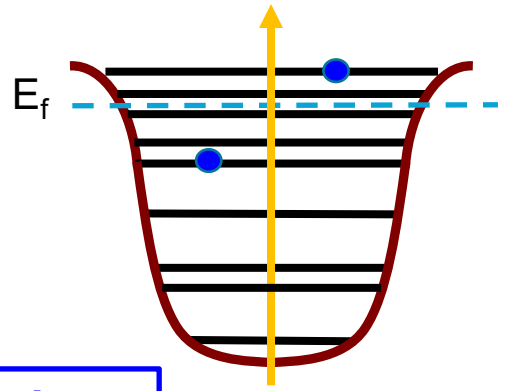

3D Lattice: no spatial symmetry restrictions

- **TDHF is based on mean-field approximation**

  TDHF gives the average number of nucleons for all reaction channels

  How to obtain the nucleon number for each reaction channel?

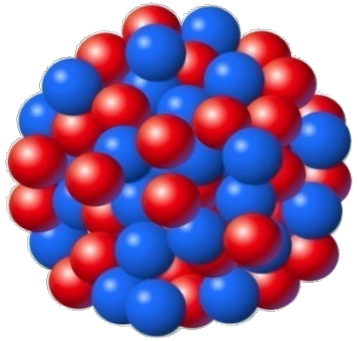

- **particle number projection method (PNP)**

  particle number projection operator:

$$\hat{P}_n = \frac{1}{2\pi}\int_0^{2\pi} d\theta e^{i(n-\hat{N}_{V_P})\theta}$$

  probability for each channel:

$$P_n = \left\langle \Psi \left| \hat{P}_n \right| \Psi \right\rangle$$

C. Simenel, Phys. Rev. Lett. **105**, 192701 (2010)

Theoretical framework for fusion evaporation reactions

Fusion evaporation reactions

$$\sigma_{\mathrm{ER}}(E_{\mathrm{c.m.}}, x) = \int_0^1 d\cos(\theta_P) \int_0^1 d\cos(\theta_T)$$

capture $\Longleftrightarrow$

$$\times \frac{\pi}{k^2} \sum_J (2J+1) T_J(E_{\mathrm{c.m.}}, \theta_T, \theta_P)$$

fusion and survival $\Longleftrightarrow$

$$\times P_{\mathrm{CN}}(\theta_P, \theta_T, E_{\mathrm{c.m.}}, J) W_{\mathrm{sur}}(E^*_{\mathrm{CN}}, x, J).$$

Theoretical framework for fusion evaporation reactions

Fusion evaporation reactions

$$\sigma_{\mathrm{ER}}(E_{\mathrm{c.m.}}, x) = \int_0^1 d\cos(\theta_P) \int_0^1 d\cos(\theta_T)$$

capture $\Longleftrightarrow$

$$\times \frac{\pi}{k^2} \sum_J (2J+1) T_J(E_{\mathrm{c.m.}}, \theta_T, \theta_P)$$

fusion and survival $\Longleftrightarrow$

$$\times P_{\mathrm{CN}}(\theta_P, \theta_T, E_{\mathrm{c.m.}}, J) W_{\mathrm{sur}}(E^*_{\mathrm{CN}}, x, J).$$

- Capture process: Schrodinger equation for penetration probability

$$\left[\frac{-\hbar^2}{2\mu}\frac{d^2}{dR^2} + \frac{J(J+1)\hbar^2}{2\mu R^2} + V_{\text{DC-FHF}}(R) - E_{\mathrm{c.m.}}\right]\psi(R) = 0$$

Theoretical framework for fusion evaporation reactions

Fusion evaporation reactions

$$\sigma_{\mathrm{ER}}(E_{\mathrm{c.m.}}, x) = \int_0^1 d\cos(\theta_P) \int_0^1 d\cos(\theta_T)$$

capture ⟺

$$\times \frac{\pi}{k^2} \sum_J (2J+1) T_J(E_{\mathrm{c.m.}}, \theta_T, \theta_P)$$

fusion and survival ⟺

$$\times P_{\mathrm{CN}}(\theta_P, \theta_T, E_{\mathrm{c.m.}}, J) W_{\mathrm{sur}}(E^*_{\mathrm{CN}}, x, J).$$

- Capture process: Schrodinger equation for penetration probability

$$\left[\frac{-\hbar^2}{2\mu}\frac{d^2}{dR^2} + \frac{J(J+1)\hbar^2}{2\mu R^2} + V_{\text{DC-FHF}}(R) - E_{\mathrm{c.m.}}\right]\psi(R) = 0$$

- Fusion Process: fusion-by-diffusion (FbD) model for fusion probability

$$P_{\mathrm{CN}}(\theta_P, \theta_T, E_{\mathrm{c.m.}}, J) = \frac{1}{2}\left[1 - \mathrm{erf}\left(\frac{\Delta V_J(\theta_P, \theta_T)}{T_J(\theta_P, \theta_T)}\right)\right],$$

Theoretical framework for fusion evaporation reactions

Fusion evaporation reactions

$$\sigma_{\mathrm{ER}}(E_{\mathrm{c.m.}}, x) = \int_0^1 d\cos(\theta_P) \int_0^1 d\cos(\theta_T)$$

capture ⟺

$$\times \frac{\pi}{k^2} \sum_J (2J+1) T_J(E_{\mathrm{c.m.}}, \theta_T, \theta_P)$$

fusion and survival ⟺

$$\times P_{\mathrm{CN}}(\theta_P, \theta_T, E_{\mathrm{c.m.}}, J) W_{\mathrm{sur}}(E^*_{\mathrm{CN}}, x, J).$$

- Capture process: Schrodinger equation for penetration probability

$$\left[\frac{-\hbar^2}{2\mu}\frac{d^2}{dR^2} + \frac{J(J+1)\hbar^2}{2\mu R^2} + V_{\text{DC-FHF}}(R) - E_{\mathrm{c.m.}}\right]\psi(R) = 0$$

- Fusion Process: fusion-by-diffusion (FbD) model for fusion probability

$$P_{\mathrm{CN}}(\theta_P, \theta_T, E_{\mathrm{c.m.}}, J) = \frac{1}{2}\left[1 - \mathrm{erf}\left(\frac{\Delta V_J(\theta_P, \theta_T)}{T_J(\theta_P, \theta_T)}\right)\right],$$

- Survival Process: statistical model for survival probability

$$W_{\mathrm{sur}}(E^*_{\mathrm{CN}}, x, J) = P(E^*_{\mathrm{CN}}, x) \prod_i^x \left(\frac{\Gamma_n(E^*_i, J)}{\Gamma_n(E^*_i, J) + \Gamma_f(E^*_i, J)}\right),$$

Fusion dynamics involving halo nuclei

PHYSICAL REVIEW C **107**, L011601 (2023)

Letter | Featured in Physics

物理亮点

Microscopic study of fusion reactions with a weakly bound nucleus: Effects of deformed halo

Xiang-Xiang Sun (孙向向) and Lu Guo (郭璐)*

School of Nuclear Science and Technology, University of Chinese Academy of Sciences, Beijing 100049, China
and CAS Key Laboratory of Theoretical Physics, Institute of Theoretical Physics, Chinese Academy of Sciences, Beijing 100190, China

How the structure of deformed halo affects the reaction dynamics?

Physics ABOUT BROWSE PRESS COLLECTIONS

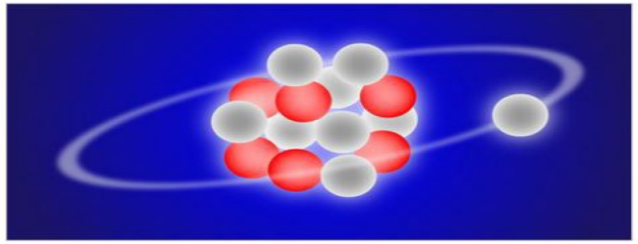

^{15}C

one-neutron halo

SYNOPSIS

Targeting a Nuclear Halo

January 4, 2023

New modeling explains the relatively high fusion reaction probabilities of halo nuclei, which are composed of a dense core surrounded by a "satellite" of one or two nucleons

Read More »

Physics SYNOPSIS

^{14,15}C+^{232}Th

Targeting a Nuclear Halo

New modeling explains the relatively high fusion reaction probabilities of halo nuclei, which are composed of a dense core surrounded by a "satellite" of one or two nucleons.

By Michael Schirber

X. X. Sun and Lu Guo, Phys. Rev. C 101, L011601 (2023); Schirber, Physics 16, s2 (2023)

Fusion dynamics involving halo nuclei

$^{14,15}C+^{232}Th$

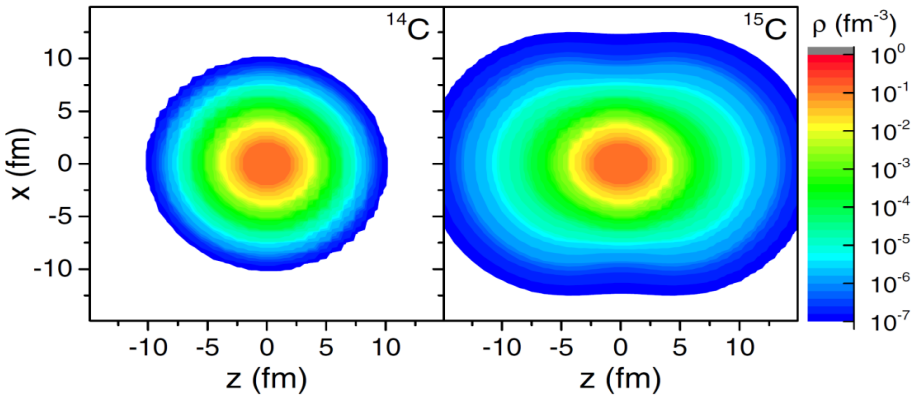

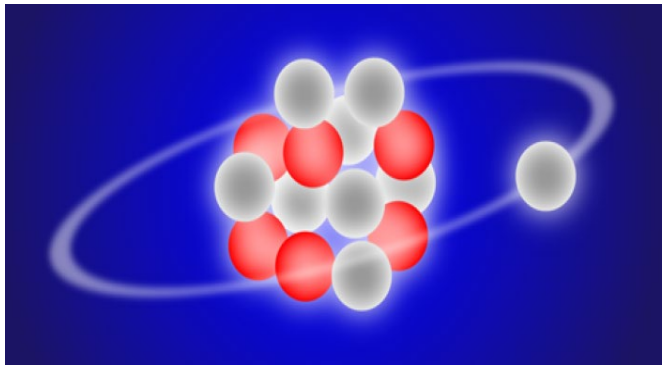

β_2 deformation

^{15}C	0.15 [Calc.]	0.14 [Refs]
^{232}Th	0.25 [Calc.]	0.26 [Exp.]

[36] H. Sagawa, X. R. Zhou, X. Z. Zhang, and T. Suzuki, Phys. Rev. C **70**, 054316 (2004).

[37] X.-X. Sun, J. Zhao, and S.-G. Zhou, Nucl. Phys. A **1003**, 122011 (2020).

- Spherical neutron magic ^{14}C, deformed one-neutron halo ^{15}C + ^{232}Th (49+14 orientations);

Fusion dynamics involving halo nuclei

$^{14,15}C+^{232}Th$

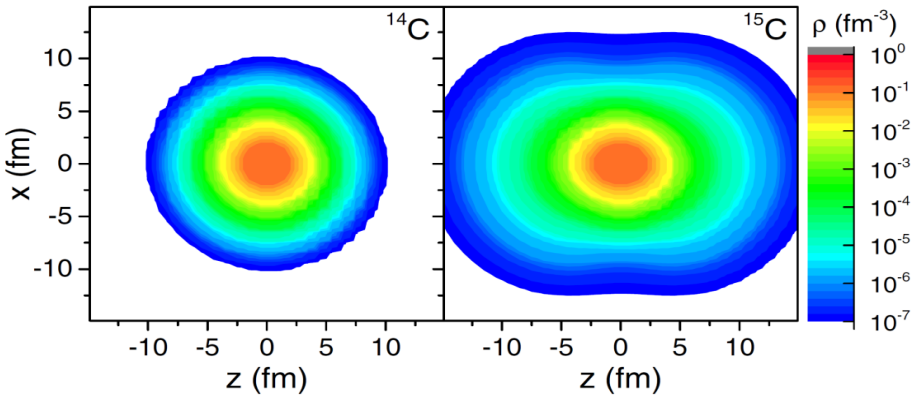

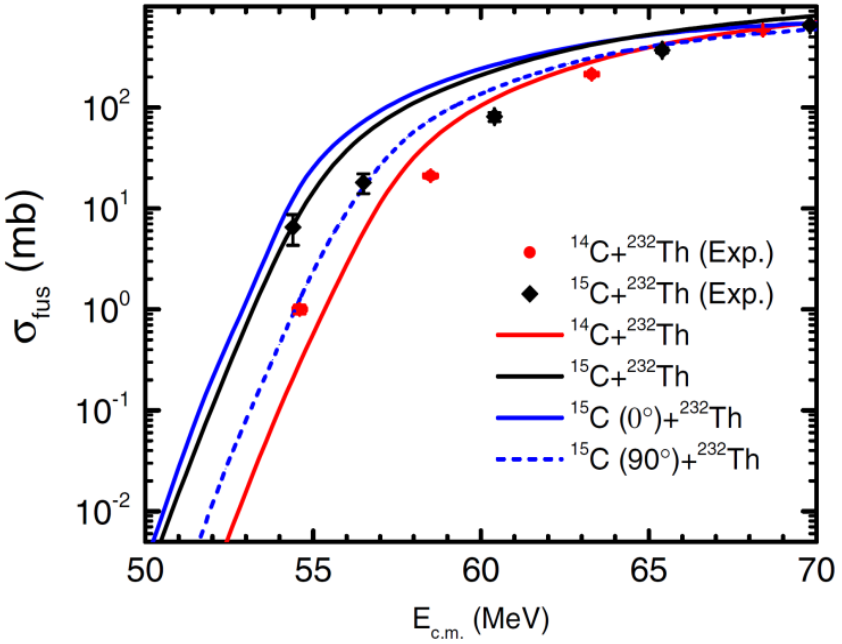

- Spherical neutron magic ^{14}C, deformed one-neutron halo ^{15}C + ^{232}Th (49+14 orientations);
- Parameter-free microscopic calculations well reproduce the enhancement of cross sections at sub-barrier;

  The underlying mechanism of this enhancement

Fusion dynamics involving halo nuclei

$^{14,15}C+^{232}Th$

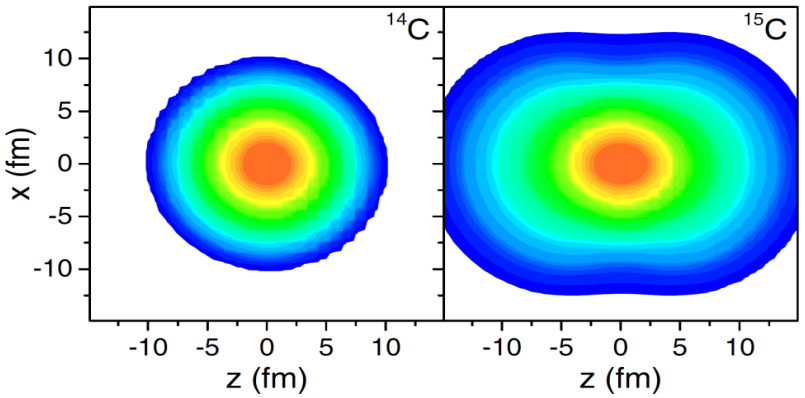

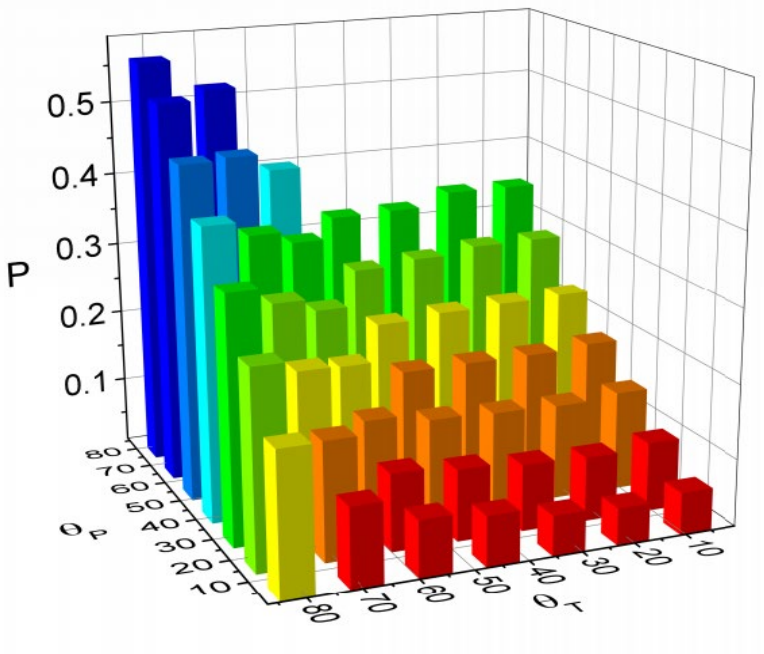

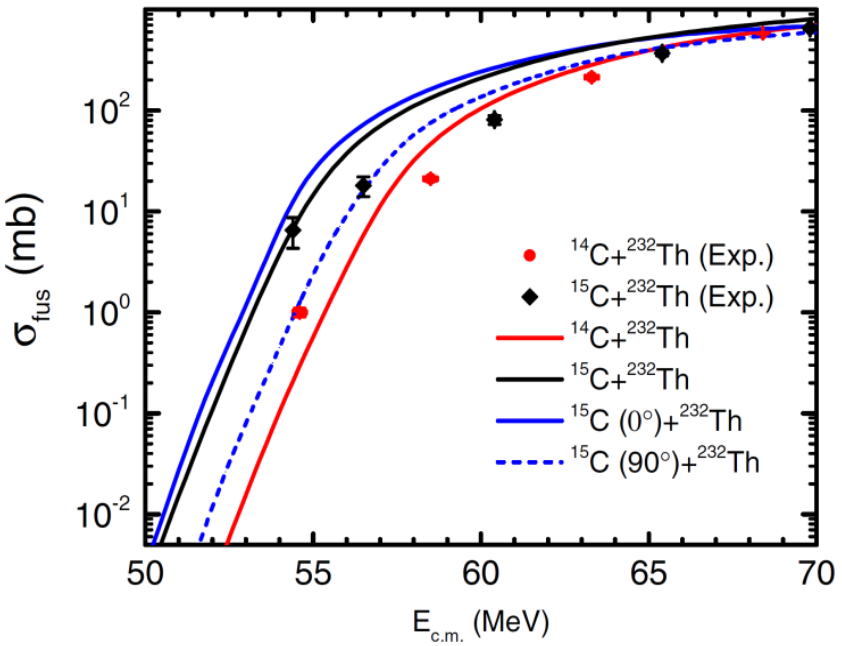

- Spherical neutron magic ^{14}C, deformed one-neutron halo ^{15}C + ^{232}Th (49+14 orientations);
- Parameter-free microscopic calculations well reproduce the enhancement of cross sections at sub-barrier;

  The underlying mechanism of this enhancement is driven by the halo structure of ^{15}C;
- One-neutron transfer channel is dominant which are more sensitive to the orientations of ^{15}C than ^{232}Th;
- Notable effect of halo structure on reaction dynamics.

Cold fusion dynamics

Compound-nucleus formation in cold-fusion reactions ^{48}Ca, ^{50}Ti, ^{54}Cr+^{208}Pb

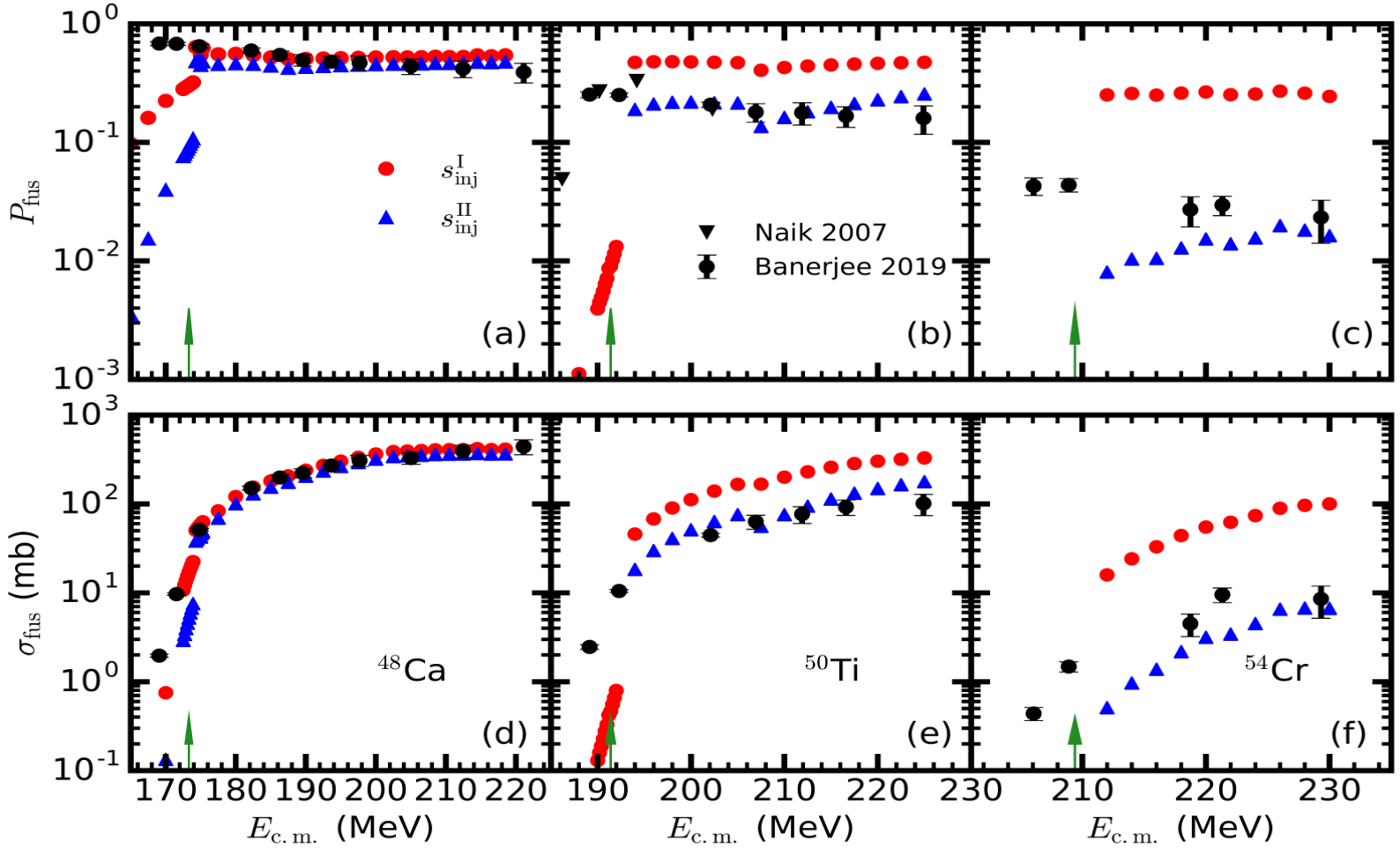

- Above the capture barrier, our calculations reproduce the measured fusion probability reasonably well.
- The restrictions from TDHF improve the predictive power of coupled-channels and diffusion calculations

X. X. Sun and Lu Guo, Phys. Rev. C 105, 054610 (2022)

Hot fusion dynamics

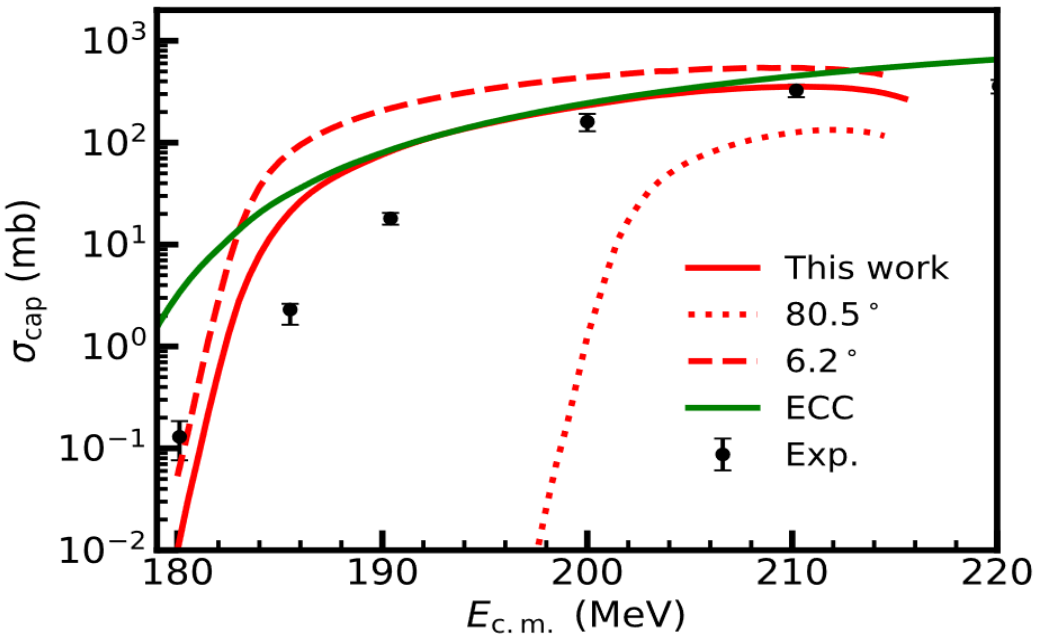

PHYSICAL REVIEW C **107**, 064609 (2023)

Editors' Suggestion

编辑推荐

Microscopic study of the hot-fusion reaction $^{48}Ca + ^{238}U$ with the constraints from time-dependent Hartree-Fock theory

Xiang-Xiang Sun (孙向向) and Lu Guo (郭璐)*

School of Nuclear Science and Technology, University of Chinese Academy of Sciences, Beijing 100049, China

and CAS Key Laboratory of Theoretical Physics, Institute of Theoretical Physics, Chinese Academy of Sciences, Beijing 100190, China

- The orientation effects of U are self-consistently included in the capture and fusion processes;
- The calculated capture cross sections agree well with the experimental data;
- The tip-orientation collision is favorable for capture;
- The capture cross sections are strongly dependent on the orientations with several orders of magnitude.

X. X. Sun and Lu Guo, Phys. Rev. C 107, 064609 (2023) Editors' Suggestions

Hot fusion dynamics

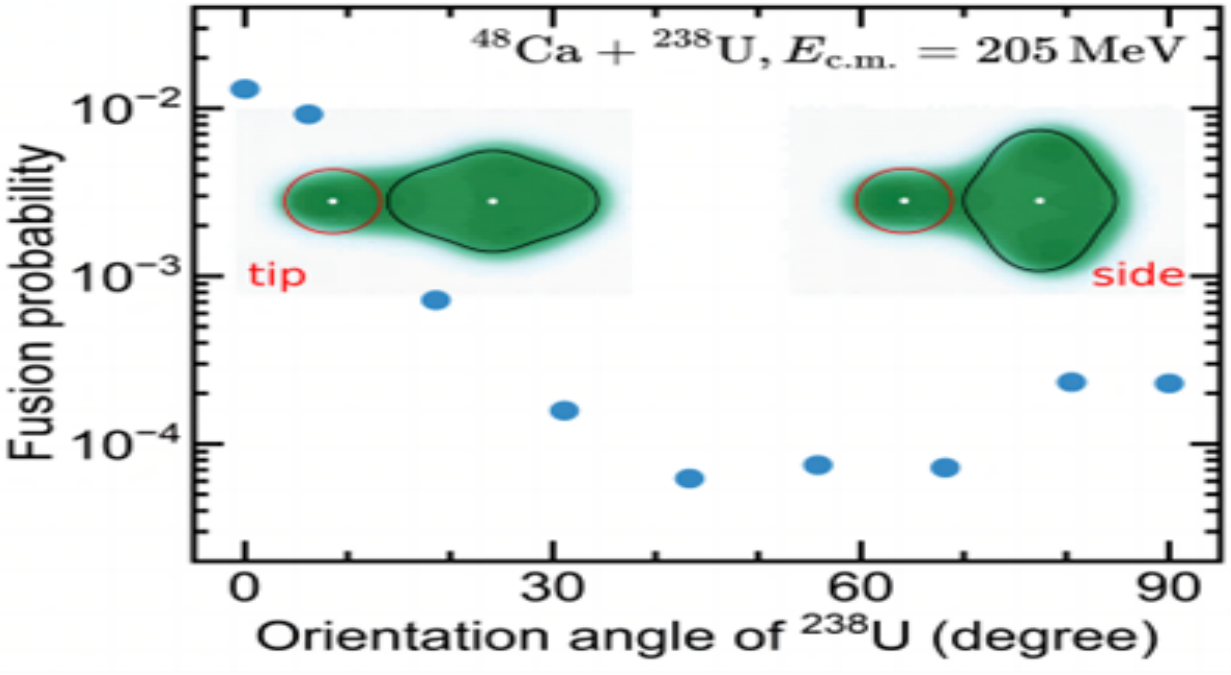

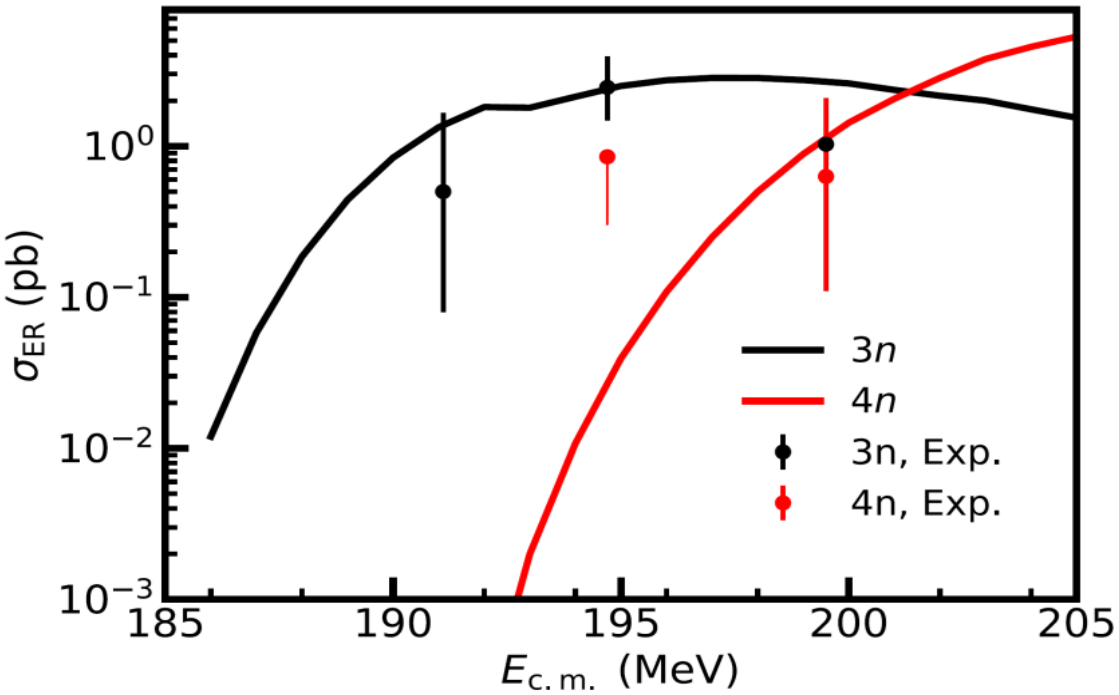

- The fusion probabilities are strongly dependent on the orientations;
- The tip-orientation collision is favorable for the formation of compound nucleus;
- The microscopic reproduce the experimental evaporation-residue cross sections.

X. X. Sun and Lu Guo, Phys. Rev. C 107, 064609 (2023)

Part II: quasifission

Quasifission dynamics

Quasifission is the main reaction channel hindering the compound nucleus formation

Key question: what is the most dominant driving mechanism in determining mass and charge of QF fragments?

^{40,48}Ca+^{238}U PRL113,182502 (2014)

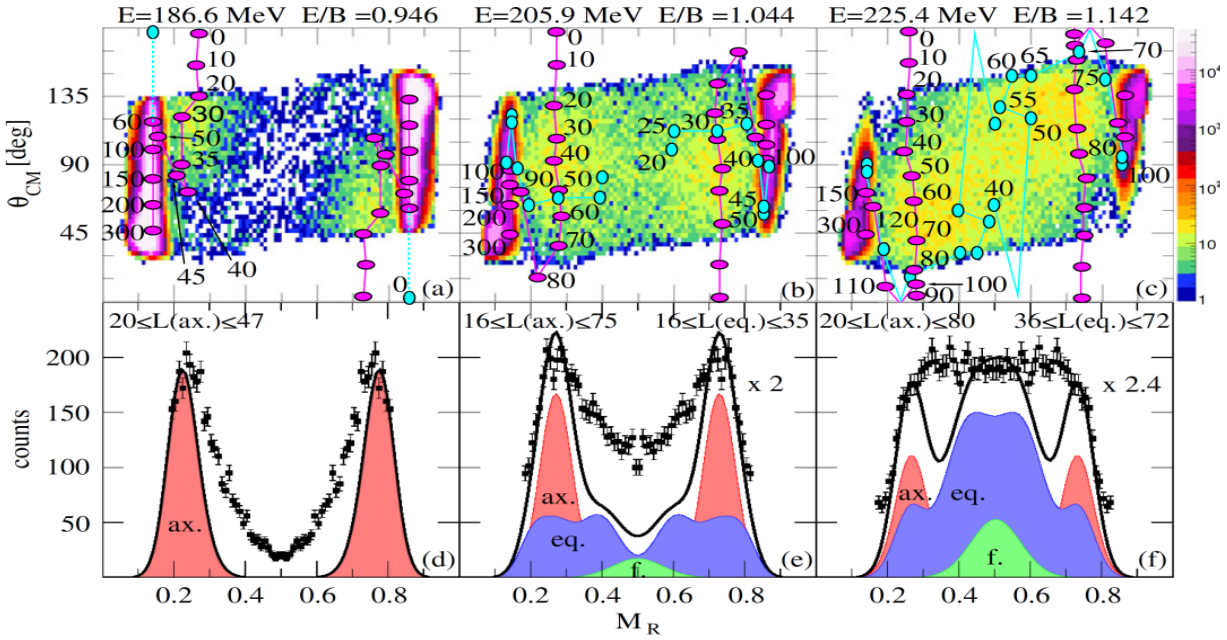

^{48}Ti+^{238}U PRL119,222502 (2017)

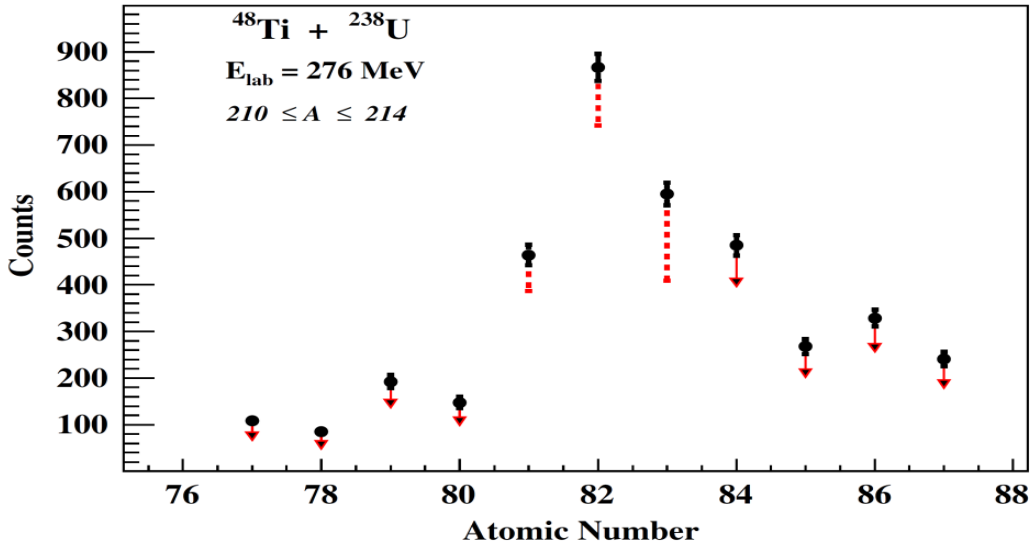

FIG. 5. Atomic number distribution for the quasifission fragments with $210 \leq A \leq 214$ (see the text for details).

- Initially the experimental mass-yield measurements indicate driving factor of shell effects;
- To unambiguously confirm shell effects, proton and neutron numbers distributions have to be measured;
- Atomic number distribution in the fragments have been measured, confirming the role of Z=82 magic shell;

Quasifission dynamics

First evidence for the impact of tensor force on the dynamical shell effects

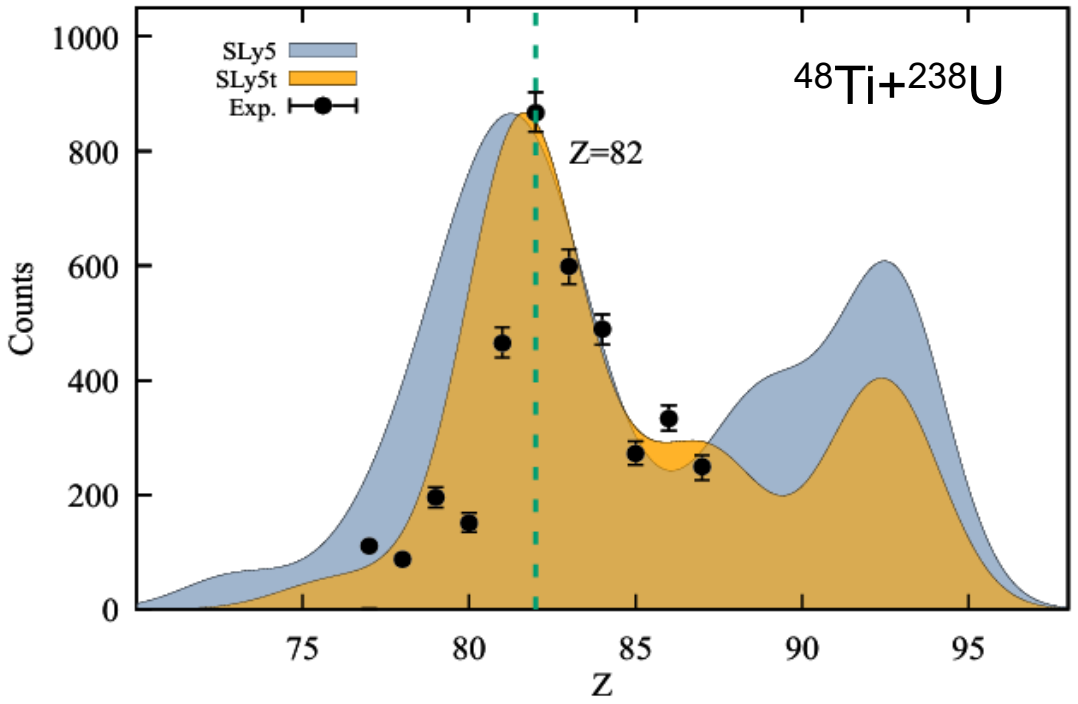

FIG. 9. Charge distribution for the quasifission reactions of ^{48}Ti + ^{238}U using the SLy5 and SLy5t forces. The experimental data is from [26].

$$\sigma_\lambda \propto \int_{b_{\min}}^{b_{\max}} b\,\mathrm{d}b \int_0^{\frac{\pi}{2}} \mathrm{d}\beta \sin(\beta) P_b^{(\lambda)}(\beta) \ ,$$

- parameter-free microscopic TDHF study;
- charge distribution shows much better agreement with experiments for SLy5t (tensor force included)
- peak position shifts and the width becomes narrower;
- prominent effects of tensor force on QF dynamics

L. Li, Lu Guo, K. Godbey, A. S. Umar, Phys. Lett. B 833,137349 (2022)
Z. J. Wu, Lu Guo, Zhong Liu, GX Peng, Phys. Lett. B 825, 136886 (2022)
L. Li, Lu Guo, K. Godbey, A. S. Umar, Phys. Rev. C 110, 064607 (2024)
Z. J. Wu and Lu Guo, , Phys. Rev. C 113, 024618 (2026)

Quasifission dynamics

First evidence for the impact of tensor force on the dynamical shell effects

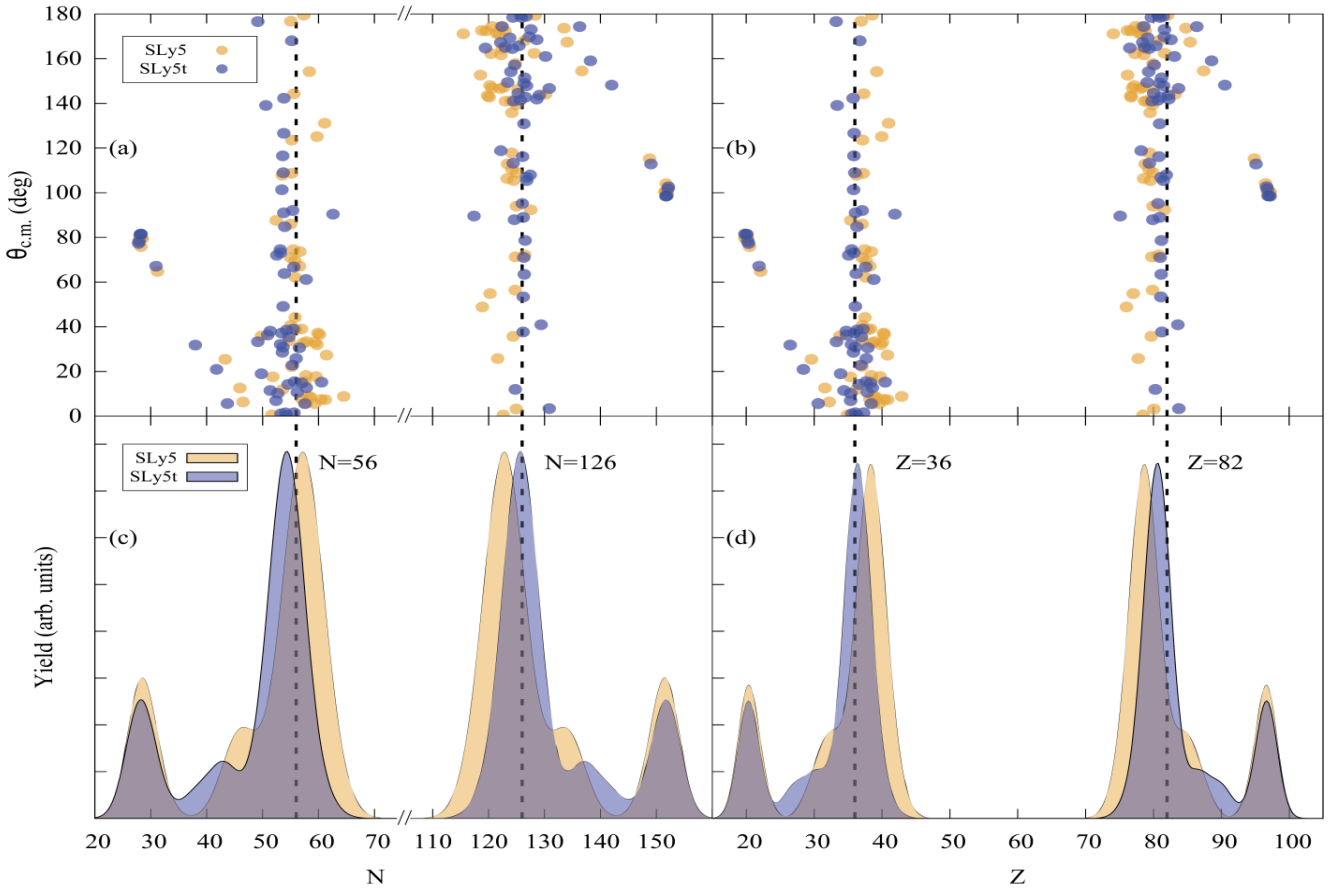

$^{48}Ca+^{249}Bk$

- The inclusion of tensor force causes the shift from deformed to spherical shells in ^{208}Pb (122---126, 78---82);
- What is the driving mechanisms and what is the role of tensor force in the delicate balance between spherical and deformed shells?

L. Li, Lu Guo, K. Godbey, A. S. Umar, Phys. Lett. B 833,137349 (2022)

Z. J. Wu, Lu Guo, Zhong Liu, GX Peng, Phys. Lett. B 825, 136886 (2022)

L. Li, Lu Guo, K. Godbey, A. S. Umar, Phys. Rev. C 110, 064607 (2024)

Z. J. Wu and Lu Guo, , Phys. Rev. C 113, 024618 (2026)

Quasifission dynamics

First evidence for the impact of tensor force on the dynamical shell effects

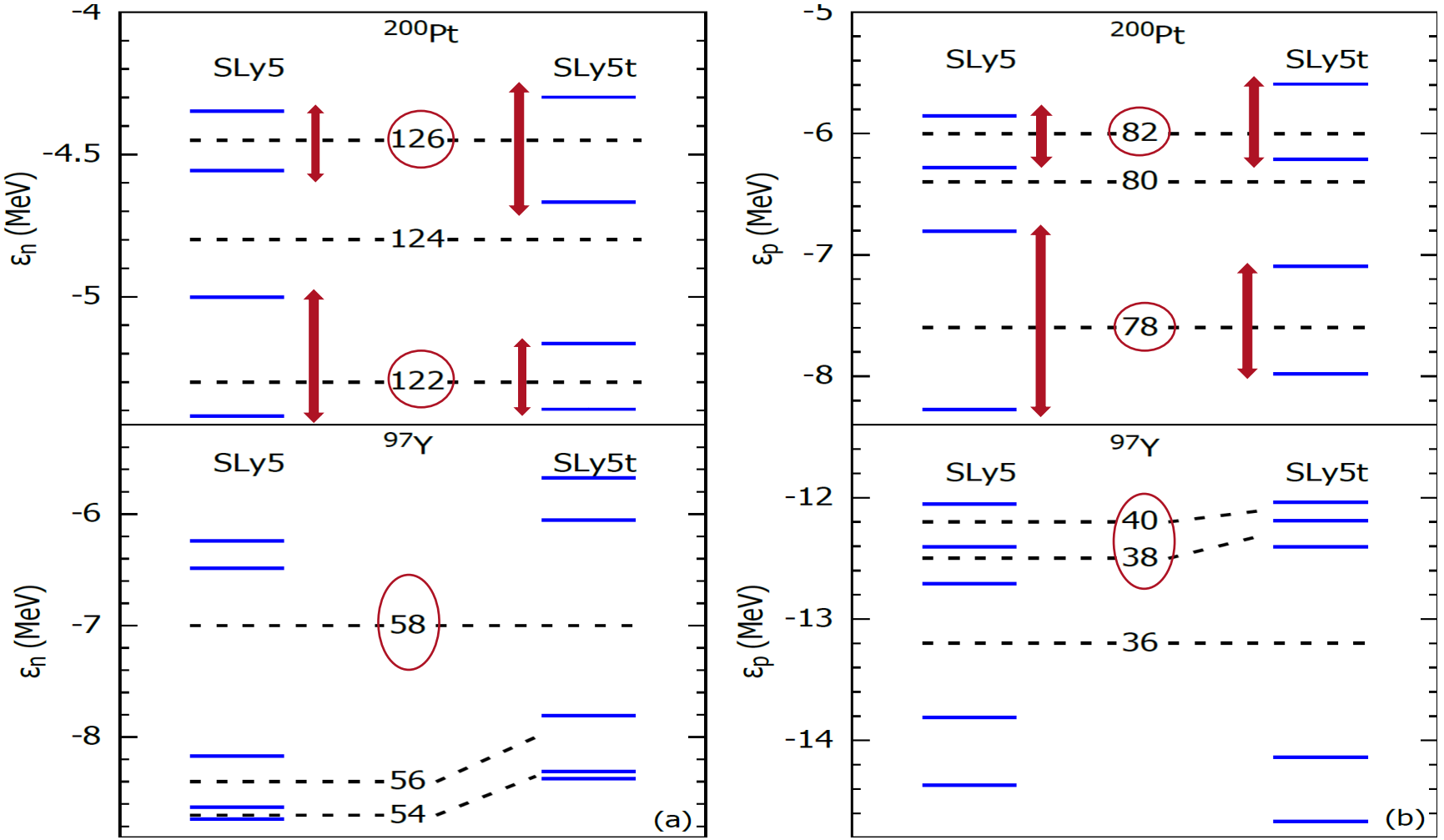

heavy fragment:

from ^{200}Pt: N=122, Z=78

to ^{208}Pb: N=126, Z=82

L. Li, Lu Guo, K. Godbey, A. S. Umar, Phys. Lett. B 833,137349 (2022)

L. Li, Lu Guo, K. Godbey, A. S. Umar, Phys. Rev. C 110, 064607 (2024)

Quasifission dynamics

Systematic studies of quasifission in hot fusion systems for synthesizing SHE with Z=112-120;

All the reactions producing 119 and 120 in the world; the reactions using ^{48}Ca, ^{50}Ti, ^{54}Cr projectiles;

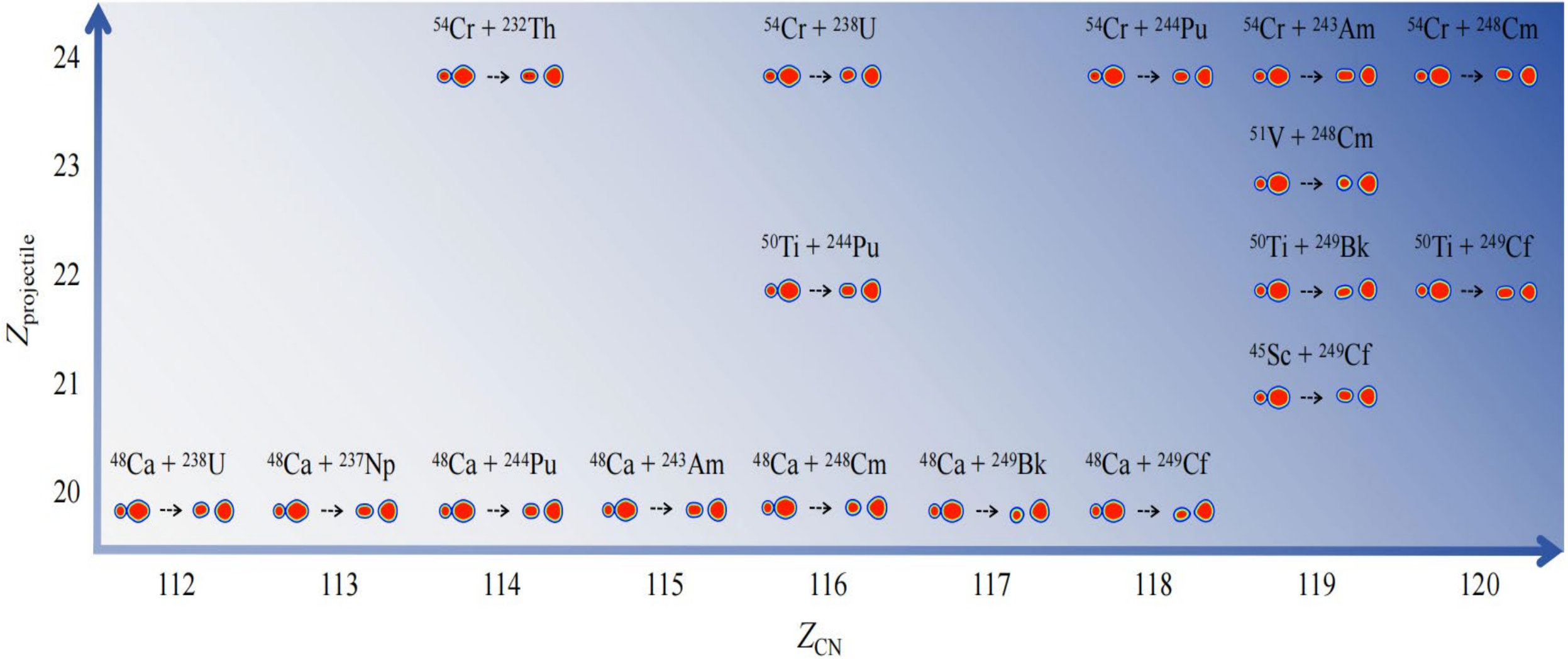

Quasifission dynamics

- Charge and neutron number of QF fragments;
- Importance of spherical quantum shells in ^{208}Pb (Z=82, N=126);

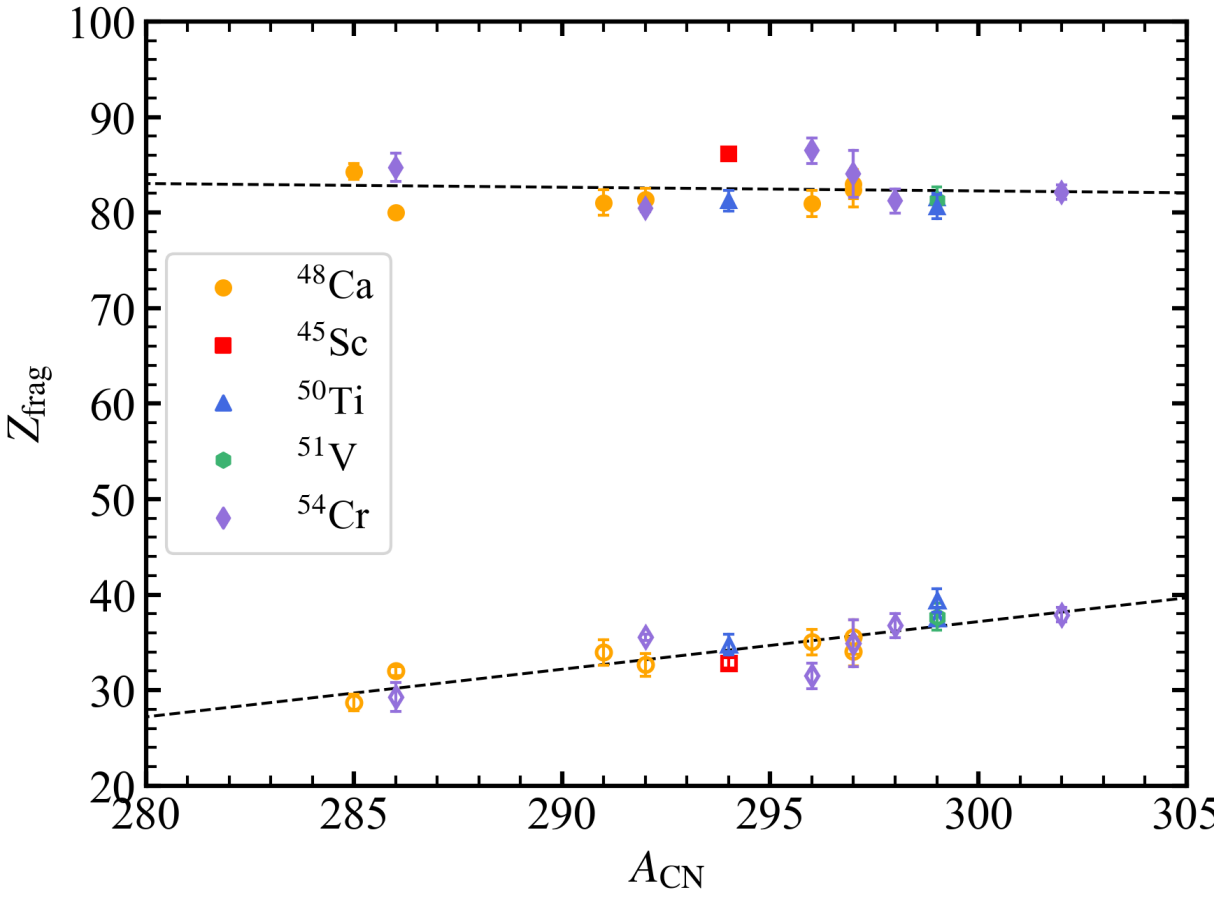

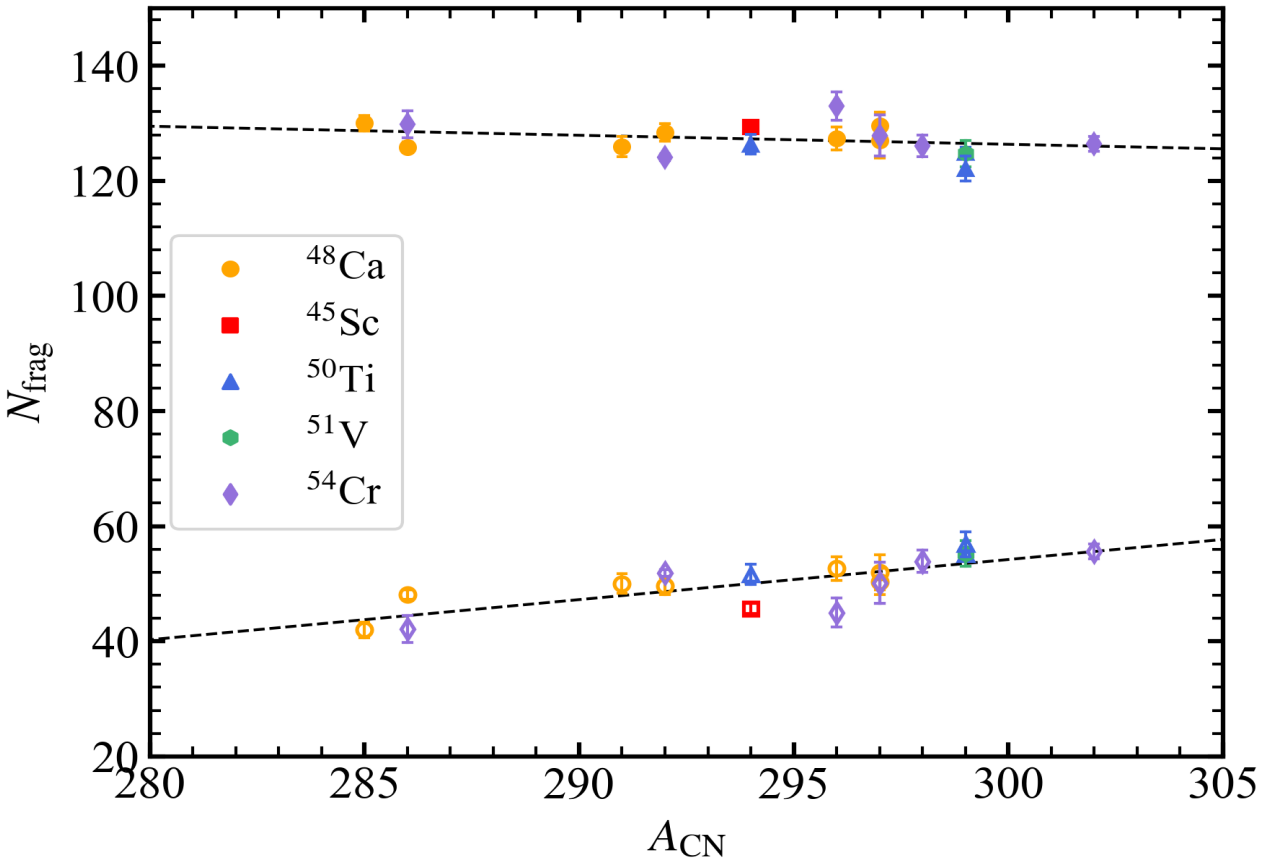

Part III: fission

Theoretical model for fission

- Nuclear fission is a complex nonequilibrium process due to the transitions between the motion of mother nucleus…
- The theoretical description of induced fission is divided into two phases:
  - The ground state transits to a configuration beyond the fission barrier: adiabatic process, e.g. HFB, HF+BCS
  - Fast evolution of neck rupture: nonadiabatic process, e.g. TDDFT

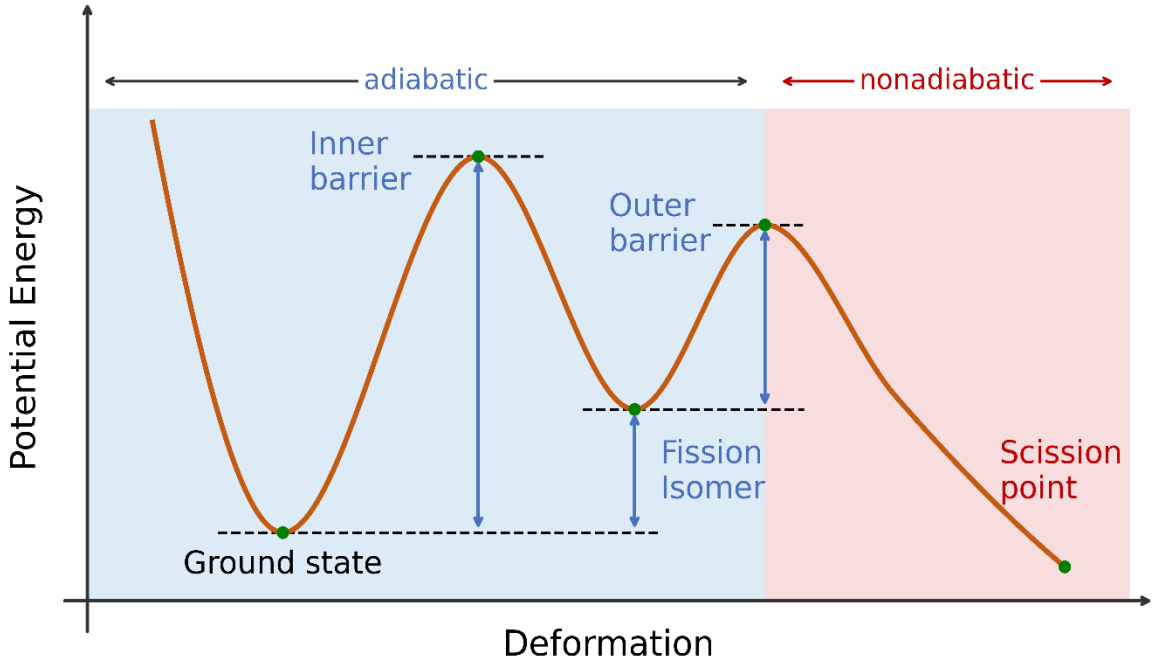

Fission dynamics with TDDFT:

- Quantum shell effect for the formation of fission fragments
- Odd-even effect in the charge distribution of fission fragments
- A way to give the proper mass and charge distributions
- Effect of tensor force in dynamics

Fission dynamics

HF+BCS in 3D lattice on Q20, Q30, Q22

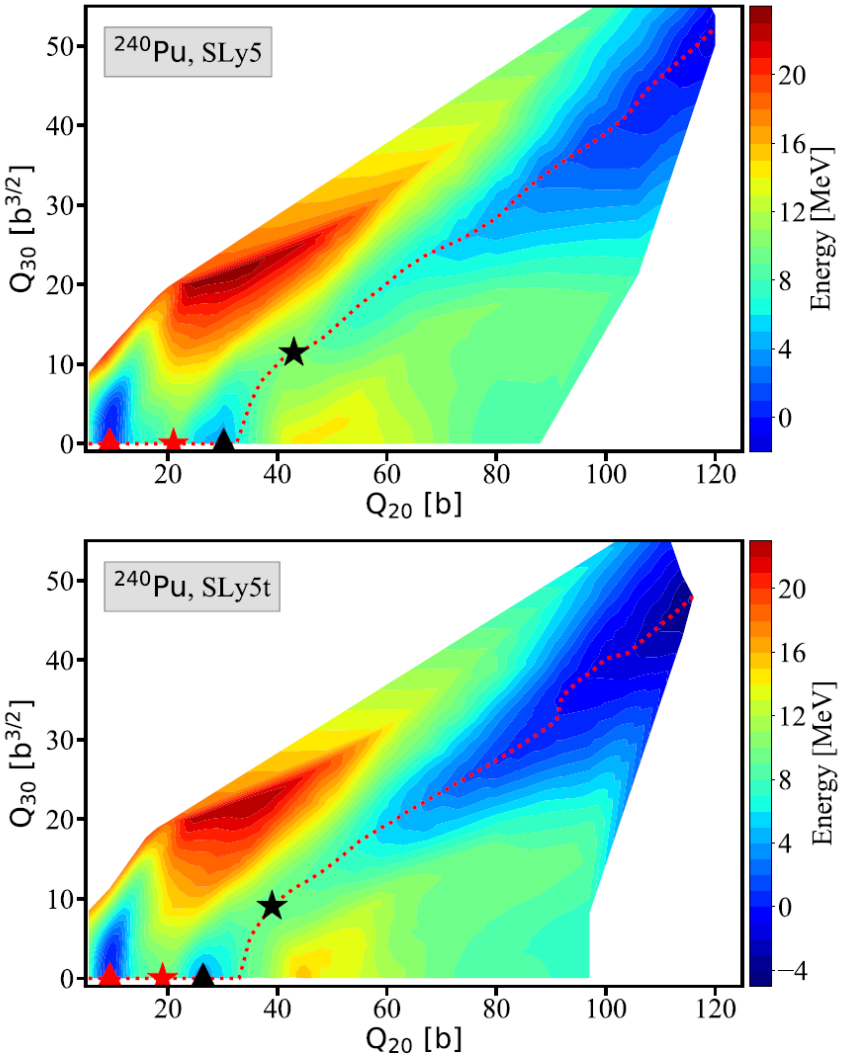

- The tensor force in SLy5t is perturbatively added based on SLy5
- Beyond B_0, fission valley is apparently enlarged by the tensor force.

  Such a broad fission valley may be favored for dynamical evolution.

Y. Huang, X. X. Sun, and Lu Guo, Phys. Rev. C 110, 064318 (2024), Eur. Phys. J. A 60, 100 (2024);

Fission dynamics

HF+BCS in 3D lattice on Q20, Q30, Q22

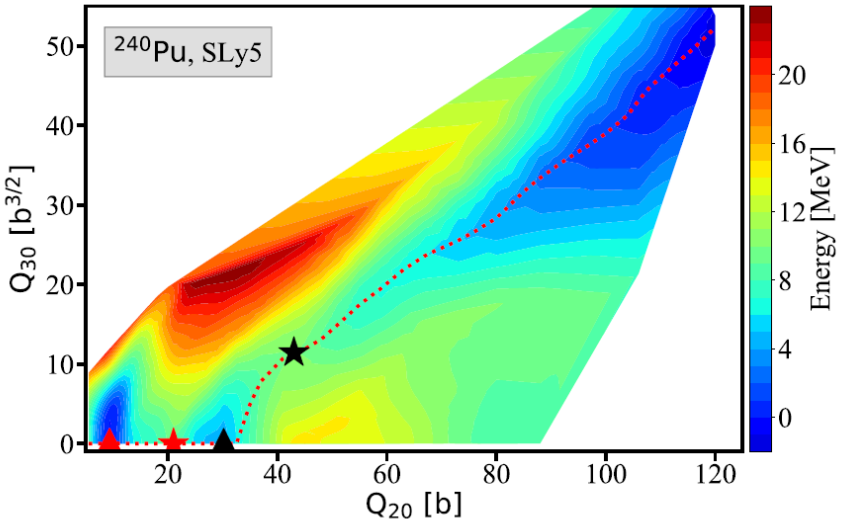

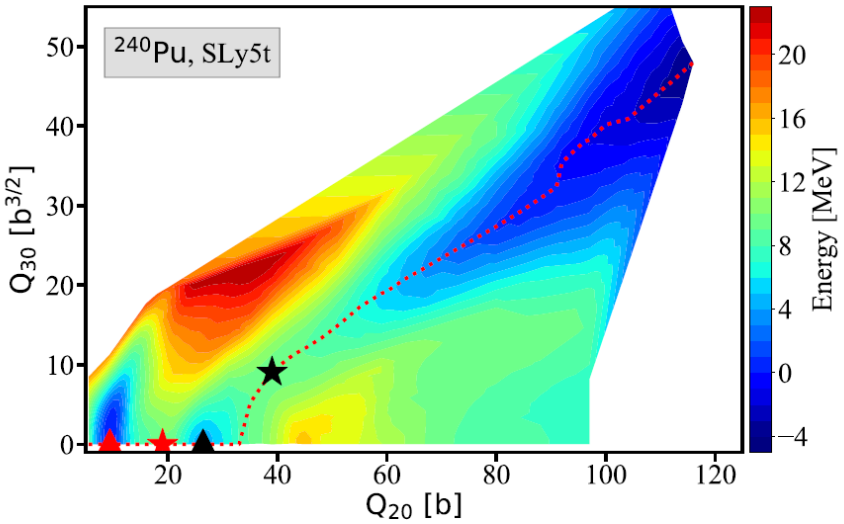

- The tensor force in SLy5t is perturbatively added based on SLy5
- Beyond B_o, fission valley is apparently enlarged by the tensor force.
  Such a broad fission valley may be favored for dynamical evolution.
- Static fission path, ground state, inner barrier, isomeric state, and outer barrier for deformation, GS unchanged, the three B_i, B_{is}, B_o becomes smaller with tensor
- For barrier height, higher inner barrier and lower outer barrier with tensor force
- Triaxial def. occurs at B_i, B_o; this observation that… is consistent with…

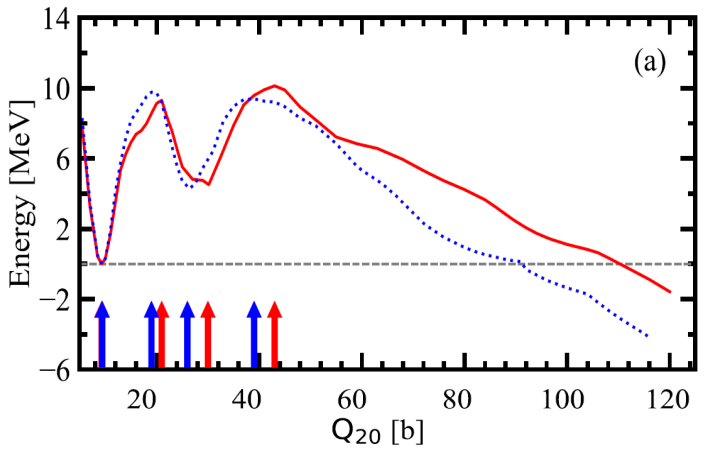

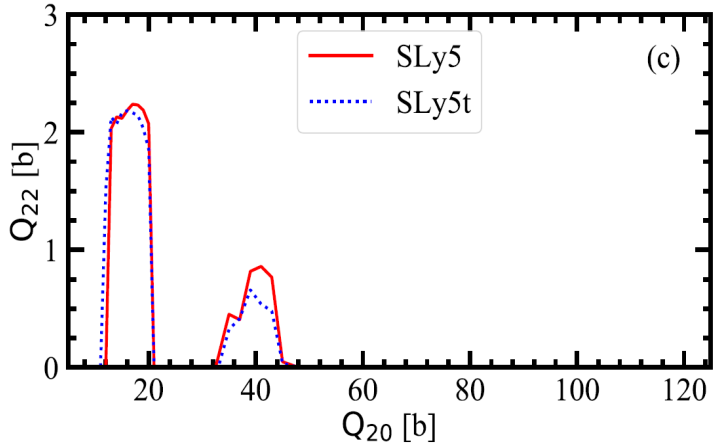

Y. Huang, X. X. Sun, and Lu Guo, Phys. Rev. C 110, 064318 (2024), Eur. Phys. J. A 60, 100 (2024);

Fission dynamics

TDDFT nonadiabatic dynamics of fission

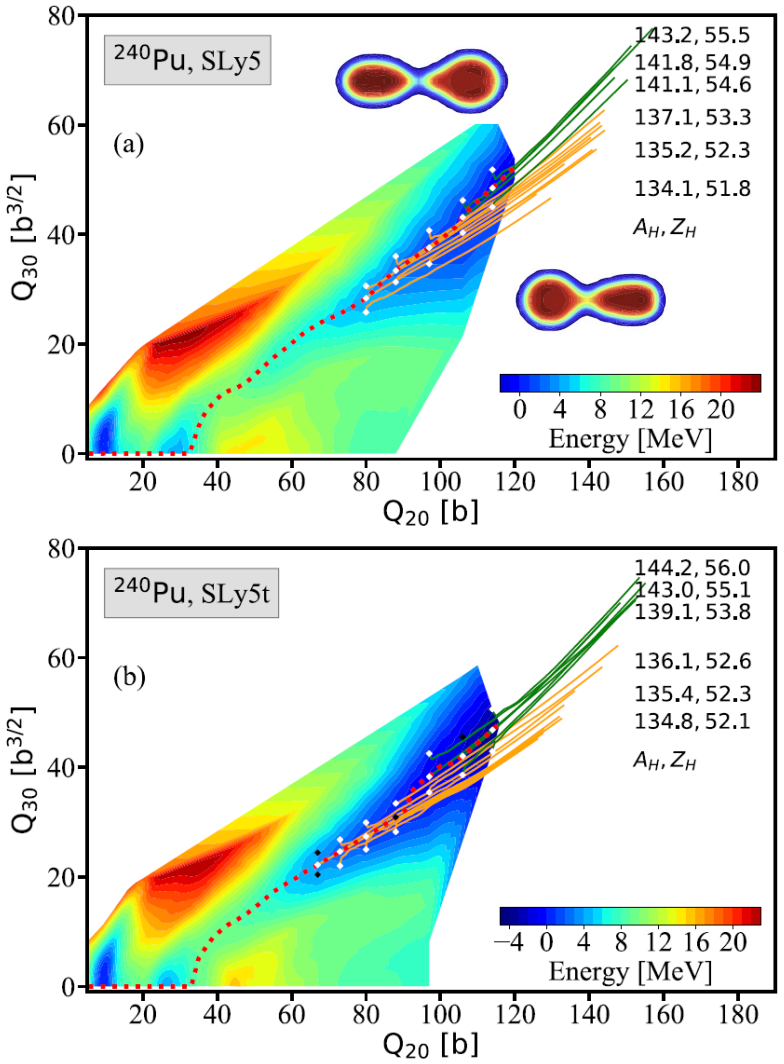

- Beyond B_o, the 15 states with equal distance along the static fission path with excitation energy 2.1 MeV and variance of 3 MeV
- Q30 of dynamical fission trajectories increases with the elongation
- Mass and charge of heavy fragments, two kinds of dynamical path

  A_H ~ 135 and Z_H ~52 in yellow, A_H ~ 142 and Z_H ~55 in green

  SI and SII channels in Brosa model

Y. Huang, X. X. Sun, and Lu Guo, Phys. Rev. C 110, 064318 (2024), Eur. Phys. J. A 60, 100 (2024);

Fission dynamics

TDDFT nonadiabatic dynamics of fission

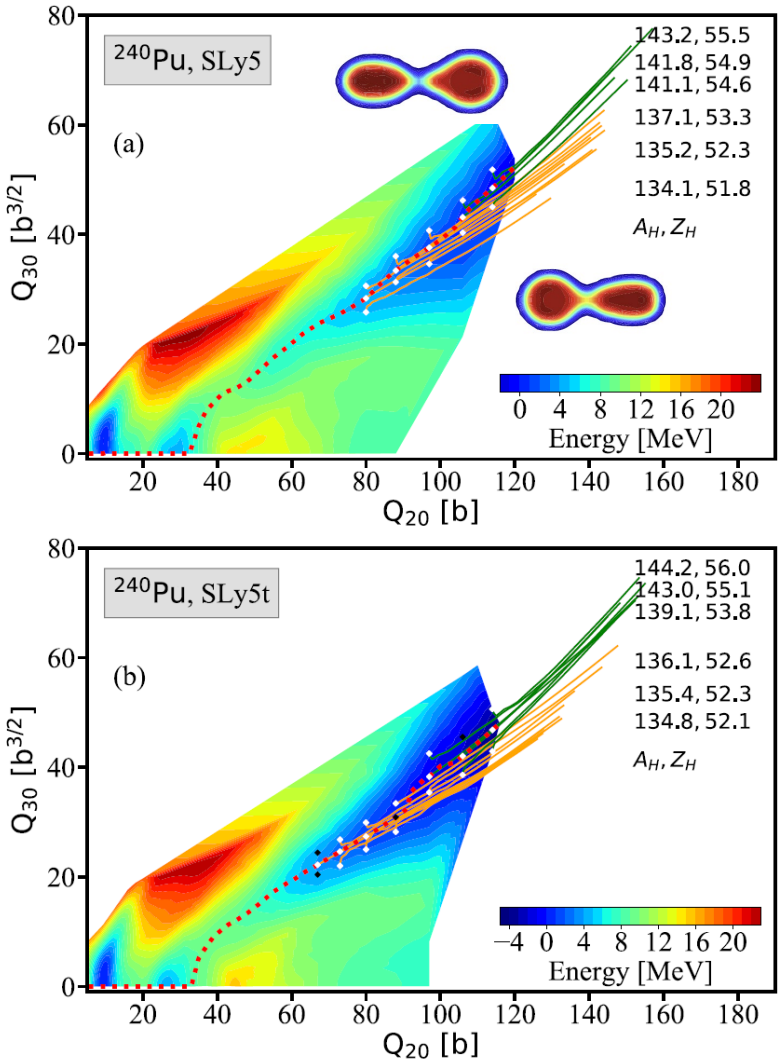

- Beyond B_o, the 15 states with equal distance along the static fission path with excitation energy 2.1 MeV and variance of 3 MeV
- Q30 of dynamical fission trajectories increases with the elongation
- Mass and charge of heavy fragments, two kinds of dynamical path

  A_H ~ 135 and Z_H ~52 in yellow, A_H ~ 142 and Z_H ~56 in green

  SI and SII channels in Brosa model
- Mean value of AH ZH in two channels are very close, while their Δ are quite differen

  For SI channel in SLy5t smaller Δ, in SII channel larger, indicating heavy fragments near 135 become concentrated and around 142 are more dispersed with tensor

	SI channel				SII channel			
Force	$\bar{A}_H$	ΔA_H	$\bar{Z}_H$	ΔZ_H	$\bar{A}_H$	ΔA_H	$\bar{Z}_H$	ΔZ_H
SLy5	135.2	0.90	52.3	0.45	142.4	0.94	55.1	0.36
SLy5t	135.5	0.43	52.4	0.19	142.3	2.40	55.1	0.93

Y. Huang, X. X. Sun, and Lu Guo, Phys. Rev. C 110, 064318 (2024), Eur. Phys. J. A 60, 100 (2024);

Fission dynamics

Localization Function along static fission path

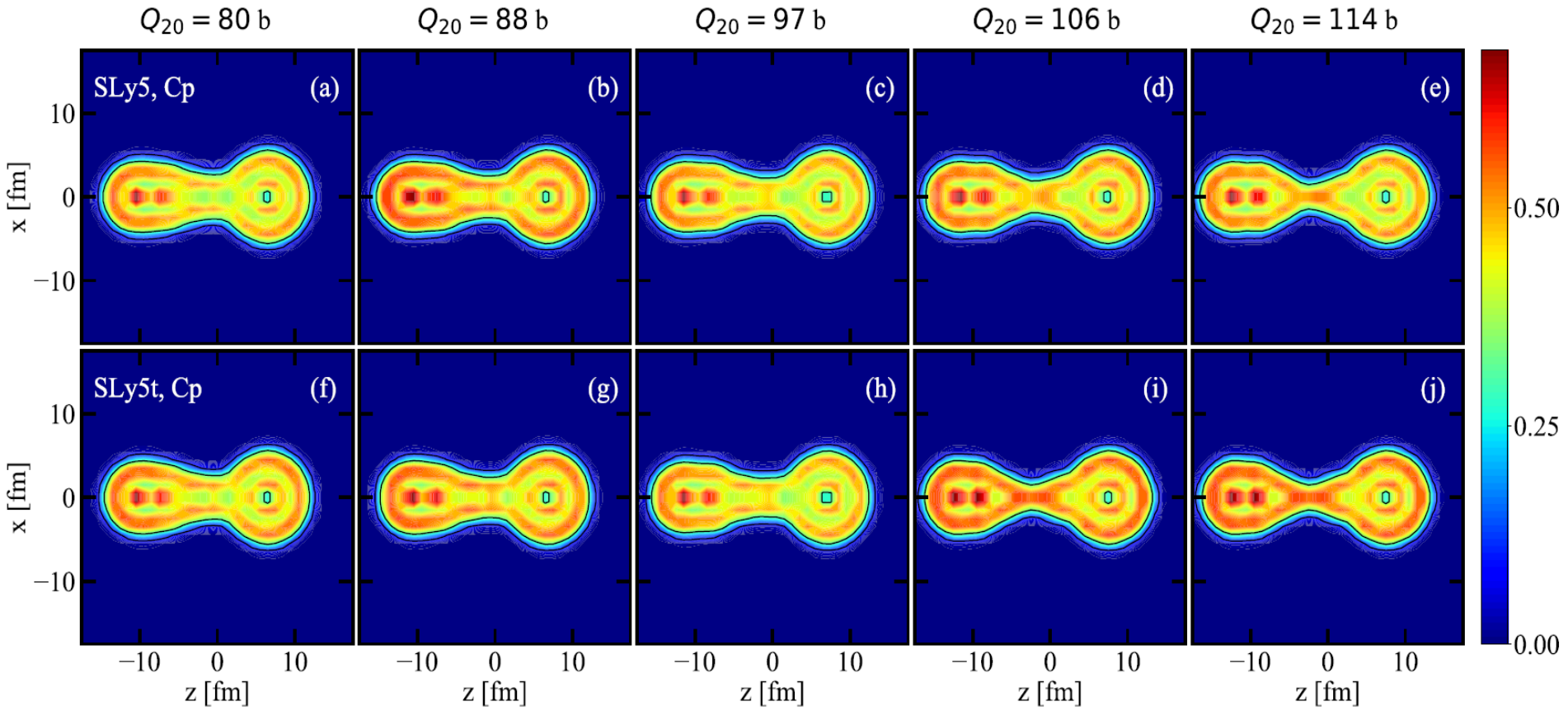

- Tensor effect on the internal structure of initial states, NLF is shown
- The shell structure is enhanced in initial configuration with the tensor

Y. Huang, X. X. Sun, and Lu Guo, Phys. Rev. C 110, 064318 (2024), Eur. Phys. J. A 60, 100 (2024);

Fission dynamics

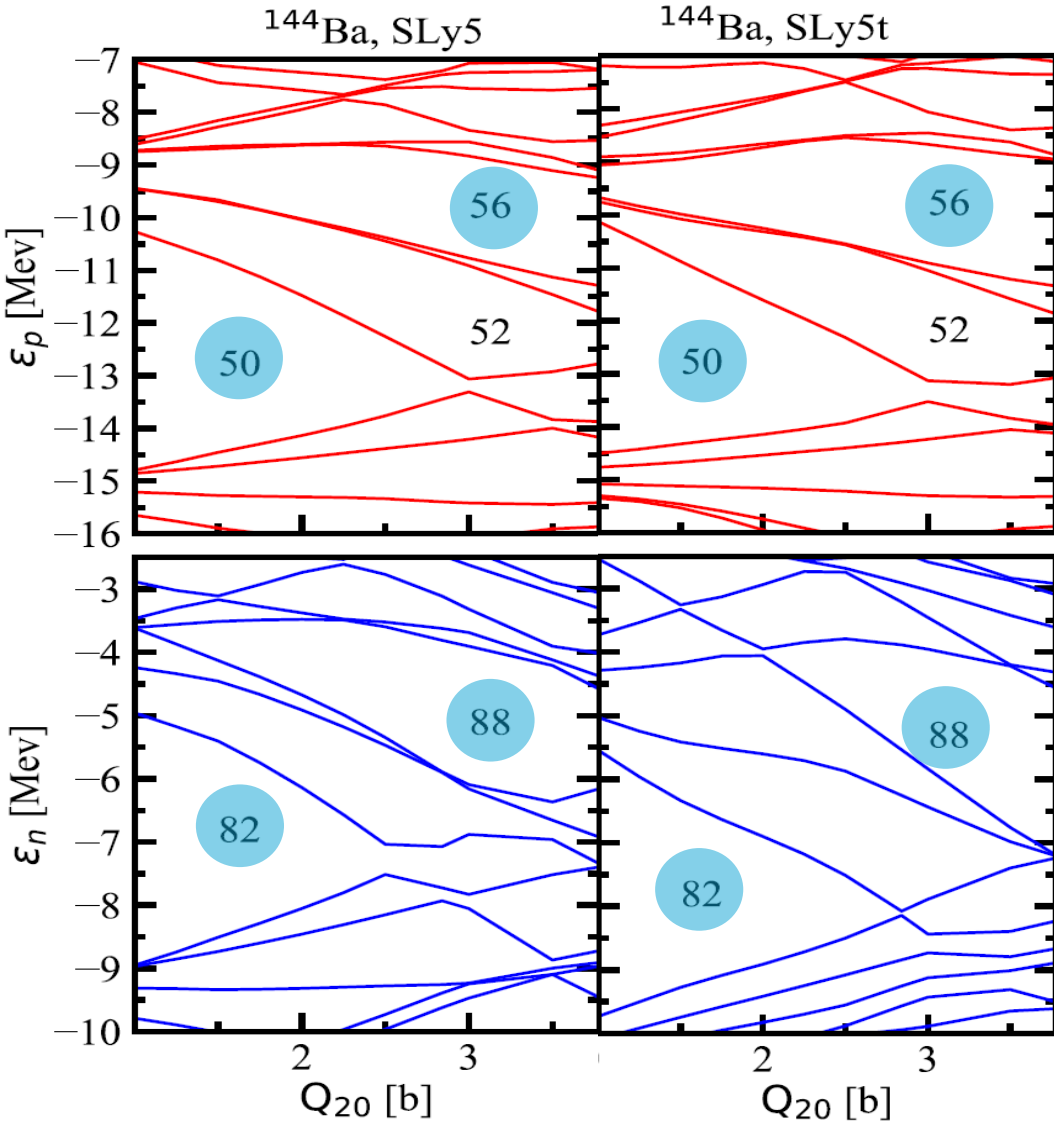

Key question: what is the most dominant driving mechanism in determining mass and charge of fission fragments?

- the evolution of SPLs as an increase of *Q*20 up to scission point.
- for SPLs of protons (neutron), as *Q*20 increases, the sph. shell *Z*=50 (N=82) is quenched and the def. shell gaps at *Z* = 52, 56 (N=88) gradually play a role.
- By including tensor force, a slight enhancement of *Z* = 56 and N=88 are observed

Y. Huang, X. X. Sun, and Lu Guo, Phys. Rev. C 110, 064318 (2024), Eur. Phys. J. A 60, 100 (2024);

Fission dynamics

TDHF with FOA + double PNP

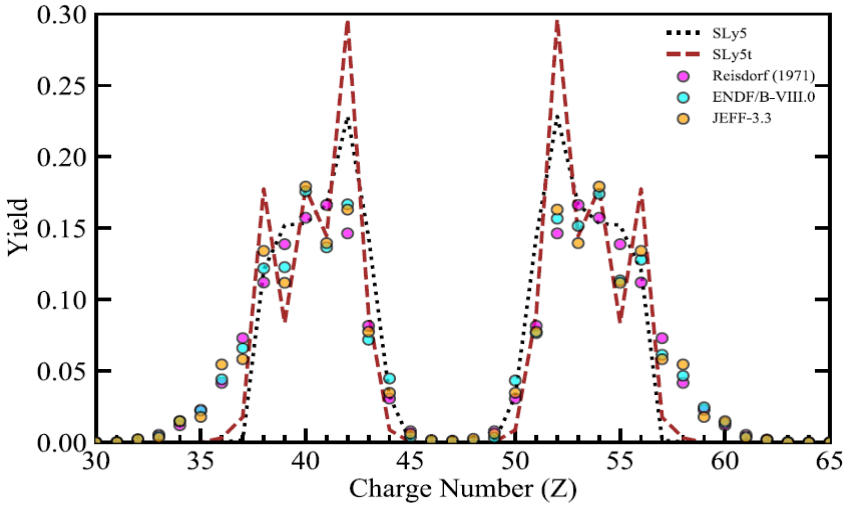

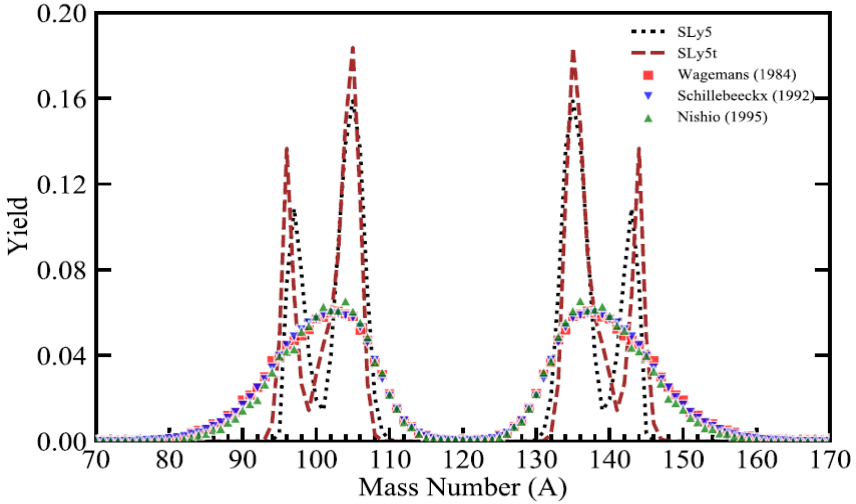

- 1st PNP: consider particle number fluctuations in the fragments

$$P_{\mathrm{V}}^{\tau}(N) \equiv \left\langle \hat{P}_{\mathrm{V}}^{\tau}(N) \right\rangle = \frac{1}{2\pi} \int_0^{2\pi} d\eta \, \langle \Psi | \, e^{i(\hat{N}_{\mathrm{V}}^{\tau} - N)\eta} | \Psi \rangle,$$

  Including pairing correlations, the overlap has a sign ambiguity problem due to the square root of a complex matrix. We adopt the Pfaffian method.

- 2nd PNP: restore the total number of particles

$$P_{\mathrm{V}}^{\tau,\,\mathrm{Double}}(N) = \frac{\langle \Psi | \, \hat{P}_{\mathrm{V}}^{\tau}(N) \hat{P}^{\tau}(N_{\mathrm{tot}}) \, | \Psi \rangle}{\langle \Psi | \, \hat{P}^{\tau}(N_{\mathrm{tot}}) \, | \Psi \rangle},$$

  For superfluid fissioning mother nucleus

- For the charge distributions, the width is consistent with the data, and the position of the peak only slightly shifts towards the symmetric side.

Y. Huang, X. X. Sun, and Lu Guo, Phys. Rev. C 110, 064318 (2024), Eur. Phys. J. A 60, 100 (2024);

Fission dynamics

TDHF with FOA + double PNP

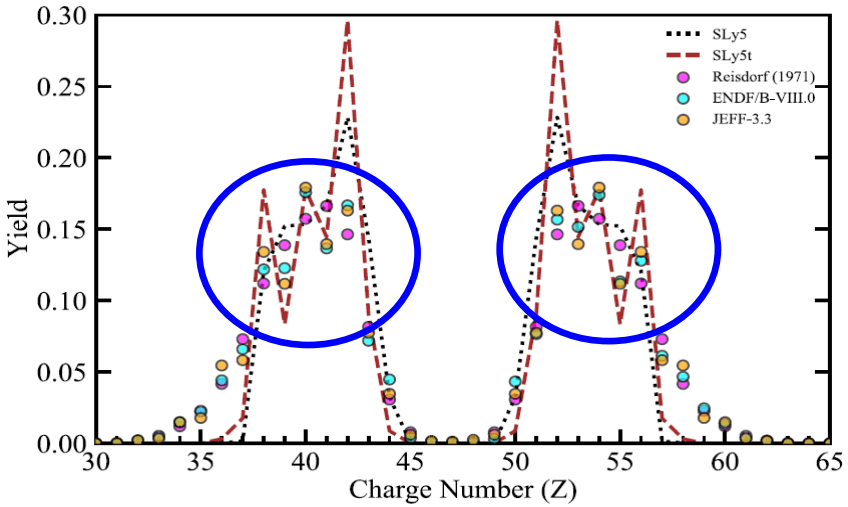

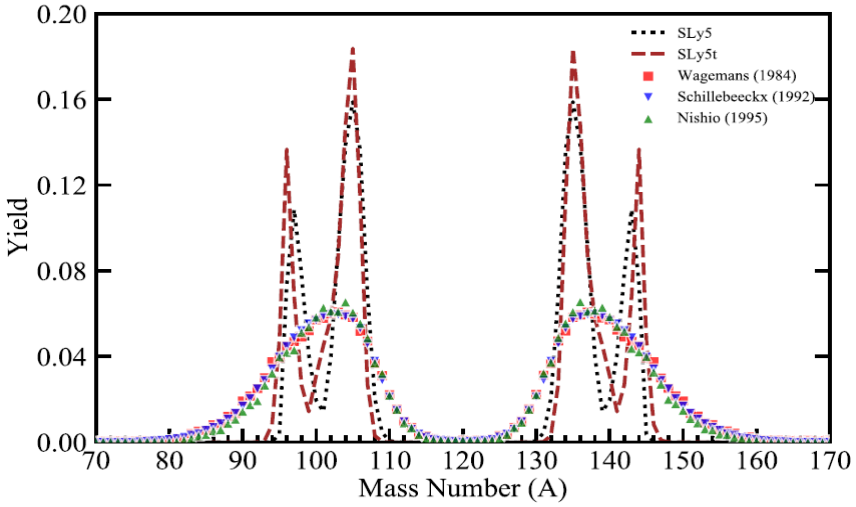

- 1st PNP: consider particle number fluctuations in the fragments

$$P_{\mathrm{V}}^{\tau}(N) \equiv \left\langle \hat{P}_{\mathrm{V}}^{\tau}(N) \right\rangle = \frac{1}{2\pi} \int_0^{2\pi} d\eta \, \langle \Psi | \, e^{i(\hat{N}_{\mathrm{V}}^{\tau} - N)\eta} | \Psi \rangle,$$

  Including pairing correlations, the overlap has a sign ambiguity problem due to the square root of a complex matrix. We adopt the Pfaffian method.

- 2nd PNP: restore the total number of particles

$$P_{\mathrm{V}}^{\tau,\,\mathrm{Double}}(N) = \frac{\langle \Psi | \, \hat{P}_{\mathrm{V}}^{\tau}(N) \hat{P}^{\tau}(N_{\mathrm{tot}}) \, | \Psi \rangle}{\langle \Psi | \, \hat{P}^{\tau}(N_{\mathrm{tot}}) \, | \Psi \rangle},$$

  For superfluid fissioning mother nucleus

- For the charge distributions, the width is consistent with the data, and the position of the peak only slightly shifts towards the symmetric side.

- clear odd-even effect in charge dis.by including tensor, peaks at even-Z;

  Referee: "This is the first microscopic model which shows the experimentally observed odd-even effect"

- Although the mass distribution is not well reproduced, a maximum yield at A_H=135 is consistent with the peak given by the experiments.

Y. Huang, X. X. Sun, and Lu Guo, Phys. Rev. C 110, 064318 (2024), Eur. Phys. J. A 60, 100 (2024);

Fission dynamics

TDHF with FOA + double PNP +GKE

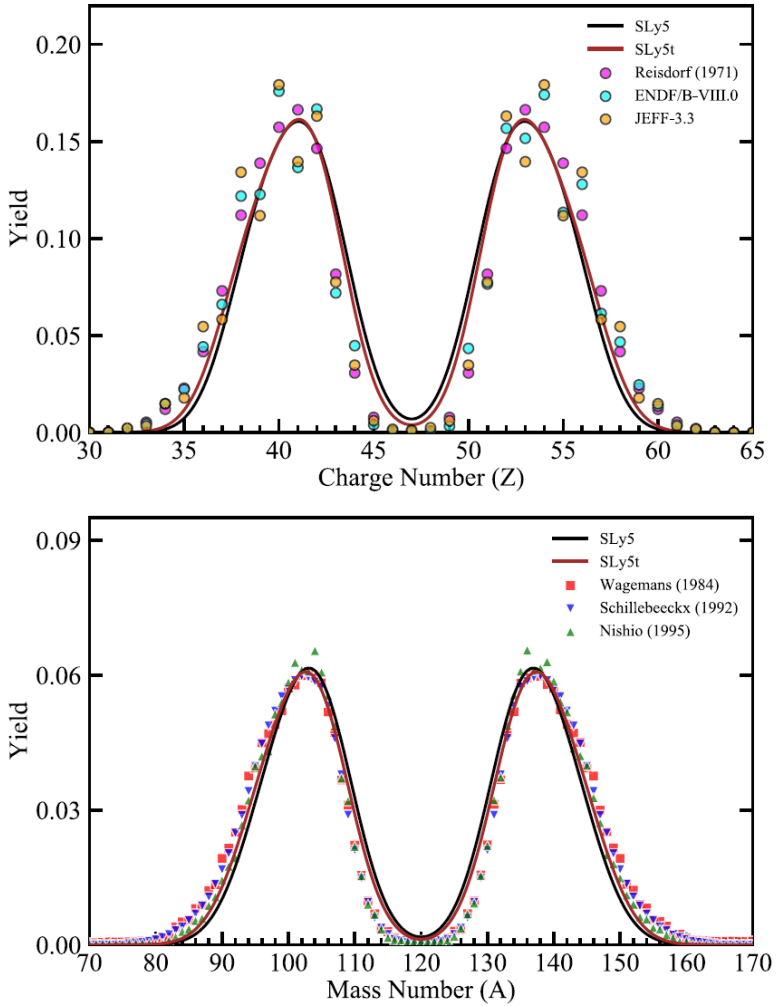

- Gaussian kernel estimation (GKE) partially make up the effects
  - The number of initial states is not enough
  - a proper weight to compensate the underestimated quantum fluctuation
- the corresponding yield well reproduces both the positions of asymmetric peaks and the widths of experiments.

Y. Huang, X. X. Sun, and Lu Guo, Phys. Rev. C 110, 064318 (2024), Eur. Phys. J. A 60, 100 (2024);

Summary and Perspectives

Summary

- Develop the microrscopic theoretical methods to study SHE production
- The fusion mechanism involving the exotic nuclei
- Cold fusion reactions and hot fusion reactions for the production of superheavy
- Quasifission mechanism and shell effects
- Multinucleon transfer reactions producing the neutron-rich nuclei
- Fission dynamics

Perspectives

- basis space, especially with pairing (TDHFB, TDHF+BCS)
- beyond the independent-particle approximation (TDRPA)
- the role of two-body collisions and fluctuation effects

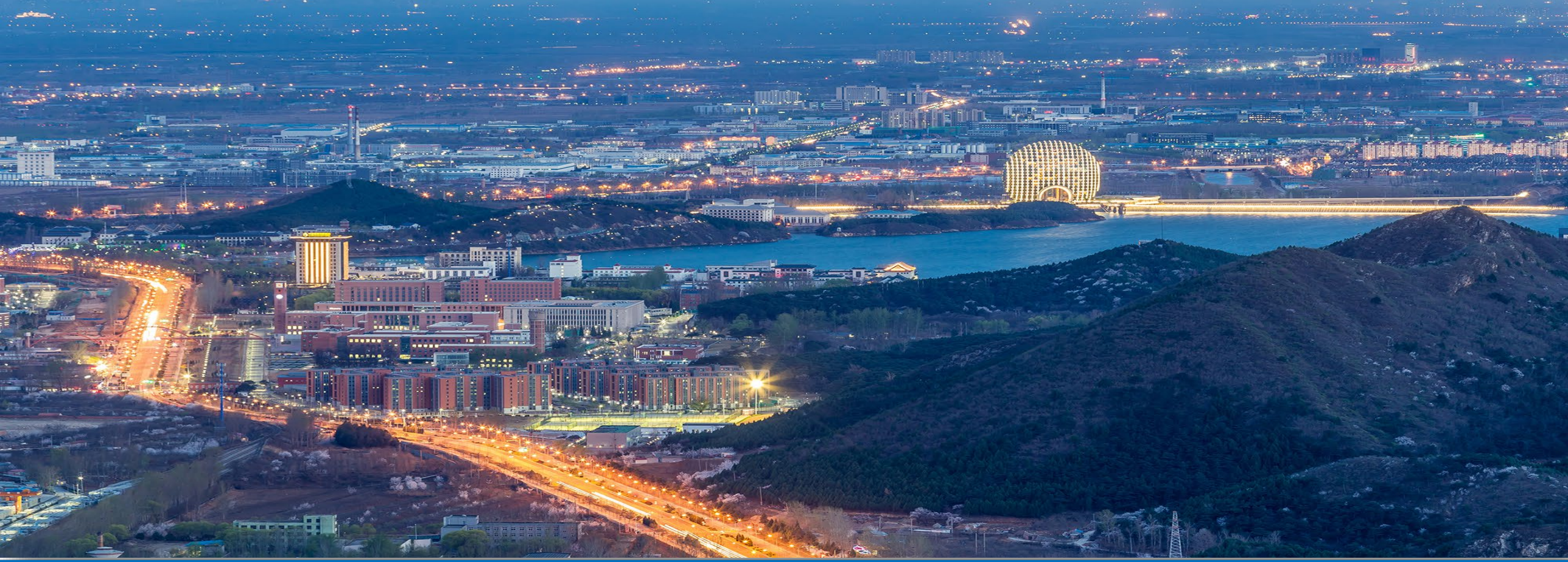

Thanks for your attention!

中国科学院大学

University of Chinese Academy of Sciences